

In vivo evaluation of the biocompatibility and biodegradation of a new denatured plasma membrane combined with liquid PRF (Alb-PRF)

Ezio Gheno , Carlos Fernando de Almeida Barros Mourão , Rafael Coutinho de Mello-Machado , Emanuele Stellet Lourenço , Richard J Miron , Karoline Ferreira Farias Catarino , Adriana Terezinha Alves , Gutemberg Gomes Alves & Mônica D. Calasans-Maia

To cite this article: Ezio Gheno , Carlos Fernando de Almeida Barros Mourão , Rafael Coutinho de Mello-Machado , Emanuele Stellet Lourenço , Richard J Miron , Karoline Ferreira Farias Catarino , Adriana Terezinha Alves , Gutemberg Gomes Alves & Mônica D. Calasans-Maia (2020): In vivo evaluation of the biocompatibility and biodegradation of a new denatured plasma membrane combined with liquid PRF (Alb-PRF), Platelets, DOI: [10.1080/09537104.2020.1775188](https://doi.org/10.1080/09537104.2020.1775188)

To link to this article: <https://doi.org/10.1080/09537104.2020.1775188>



Published online: 12 Jun 2020.



Submit your article to this journal [↗](#)



View related articles [↗](#)



View Crossmark data [↗](#)



In vivo evaluation of the biocompatibility and biodegradation of a new denatured plasma membrane combined with liquid PRF (Alb-PRF)

Ezio Gheno^{a,b}, Carlos Fernando de Almeida Barros Mourão^a, Rafael Coutinho de Mello-Machado^a, Emanuele Stellet Lourenço^a, Richard J Miron^c, Karoline Ferreira Farias Catarino^d, Adriana Terezinha Alves^e, Gutemberg Gomes Alves^f, & Mônica D. Calasans-Maia^g

^aPost-Graduation Program in Dentistry, Fluminense Federal University, Niterói, Brazil, ^bDi.S.C Department of Surgical Sciences and Integrated Diagnostics, University of Genoa, Italy, ^cDepartment of Periodontology, University of Bern, Bern, Switzerland, ^dUndergraduate Student, Dentistry School, Fluminense Federal University, Niterói, Brazil, ^eDepartment of Oral Pathology, Dentistry School, Fluminense Federal University, Niterói, Brazil, ^fDepartment of Molecular and Cell Biology, Institute of Biology, Fluminense Federal University, Niterói, Brazil, and ^gOral Surgery Department, Dentistry School, Fluminense Federal University, Niterói, Brazil

Abstract

Guided bone regeneration (GBR) is a process that involves the regeneration of bone defects through the application of occlusive membranes that mechanically exclude the population of non-osteogenic cells from the surrounding soft tissue. Interestingly, platelet-rich fibrin (PRF) has previously been proposed as an autologous GBR membrane despite its short-term resorption period of 2–3 weeks. Recent clinical observations have demonstrated that, by heating a liquid platelet-poor plasma (PPP) layer and mixing the cell-rich buffy coat zone, the resorption properties of heated albumin gel with liquid-PRF (Alb-PRF) can be significantly improved. The aim of this study was to evaluate the inflammatory reaction, biocompatibility, and extended degradation properties of a new autologous Alb-PRF membrane in comparison to commonly utilized standard PRF after nude mice implantation, according to ISO 10993–6/2016. Two standard preparations of PRF (L-PRF and H-PRF) were compared to novel Alb-PRF following subcutaneous implantation at 7, 14, and 21 days. All groups demonstrated excellent biocompatibility owing to their autologous sources. However, it is worth noting that, while both L-PRF and H-PRF membranes demonstrated significant or complete resorption by 21 days, the Alb-PRF membrane remained volume-stable throughout the duration of the study. This study demonstrates—for the first time, to the best of our knowledge—a marked improvement in the membrane stability of Alb-PRF. This indicates its future potential for use as a biological barrier membrane for GBR procedures with a long-lasting half-life, or as a biological filler material in esthetic medicine applications. Thus, further studies are warranted to explore future clinical applications in various fields of medicine.

Keywords

Alb-PRF, albumin, extended-PRF, horizontal centrifugation, platelet-rich fibrin

History

Received 2 April 2020
Revised 21 April 2020
Accepted 24 May 2020
Published online xx xxx xxx

Introduction

Guided bone regeneration (GBR) is a guided treatment where the regeneration of bone defects is obtained predictably through the application of occlusive membranes, which mechanically exclude the population of non-osteogenic cells from the surrounding soft tissue [1–3]. This facilitates the repopulation of osteogenic cells – specifically originating from the native bone – which then inhabit the bone defect, leading to new bone formation [1–3]. One of the most relevant approaches to GBR is using a membrane that coats bone tissue at the surgical site, mitigating the risk of invasion by connective tissue [2,4]. With this in mind, several resorbable and non-resorbable membranes have been used in experimental and clinical studies [1–3]. Desirable characteristics for barrier membranes used in GBR therapy include biocompatibility, cell occlusion properties, host tissue integration, and space efficiency [2,4]. While most commonly used collagen barrier membranes are resorbable, the use of

platelet-rich fibrin (PRF) has also been proposed as an alternative to the use of synthetic membranes for GBR. PRF was first described as an autologous biomaterial originating from human peripheral blood following centrifugation without additives[5]. PRF has since been utilized in many fields of medicine and regenerative dentistry, including oral surgery and implantology.⁵

Second-generation platelet concentrates induce greater healing of soft and hard tissue by increasing the concentration of growth factors, such as transforming growth factor- β (TGF- β), insulin-like growth factor 1 (IGF –1), platelet-derived growth factor (PDGF), vascular endothelial growth factor (VEGF), fibroblast growth factor (FGF), and epidermal growth factor (EGF) [5,6]. However, one of the most important issues affecting the applicability of PRF is the short local permanence of this autologous material when implanted *in vivo*[7]. Several attempts to increase the stability of this membrane at the surgical sites have been

#These authors contributed equally to this work

*Correspondence: Mônica Calasans-Maia, Niterói, RJ, Brazil monicacalasansmaia@gmail.com

undertaken by altering the centrifugation protocol, but also by combining PRF with other biomaterials which, if also autologous, could contribute to improving bone and soft tissue healing by altering membrane biodegradability [1,8–11].

In this regard, a recent study proposed a new protocol for the production of membranes, which utilized the heat treatment of the plasma layer following centrifugation to improve the working properties of PRF [12]. While the growth factor content found within PRF is typically lost during standard heating protocols, recent methods to re-incorporate liquid PRF including cells from the buffy-coat layer were proposed to favor higher cell and growth factor content (Alb-PRF). [12] Alb-PRF has since been shown to incorporate living cells with high levels of growth factor release up to 10 days or more [13]. Alb-PRF is a solid, more stable, opaque moldable membrane that has been proposed for use as a soft tissue barrier. It is also a promising biomaterial for application as a filler in oral surgery, implantology, and dermatology.

The aim of this study was to evaluate the inflammatory reaction, biocompatibility, and extended degradation properties of a new autologous Alb-PRF membrane in comparison to commonly utilized standard PRF protocols after nude mice implantation, according to ISO 10993–6/2016.

Methods

Ethical Considerations

Blood samples were collected with the informed consent of healthy volunteer donors, a procedure that was approved by the Federal Fluminense University Ethical Committee [CAAE

number 12126919.7.0000.5243] and performed following the ethical standards of the institute's ethics research committee and the 1964 Helsinki declaration. Animal breeding and experimentation were performed according to conventional guidelines of the NIH Guide for the Care and Use of Laboratory Animals, following the Brazilian Directive for the Care and Use of Animals for Scientific and Didactic Purposes - DBCA and the CONCEA Euthanasia Practice Guidelines. This study was carried out in compliance with the guidelines of the 3Rs Program (Reduction, Refinement, and Replacement), whose objective is to reduce the number of animals used during experimentation and to minimize pain and discomfort. The research protocol of this work was approved by the Ethics Committee of Animal Use from Fluminense Federal University (CEUA/UFF), under protocol number CEUA/UFF: 7190181118. This study was reported in accordance with the ARRIVE guidelines concerning relevant items [14] and supplemented by PREPARE [15].

Preparation of Control Biomaterials

In the control groups, PRF was prepared using the peripheral blood from one healthy donor (C.F.A.B.M.), collected using 9 ml red cap glass tubes, without any additives. All PRF samples in this study were collected from the same donor to limit the variability in this study, as major differences have previously been reported in this aspect [16]. The only sources of variability were the preparation of animals and the protocols followed. For the control standard protocol, leukocyte and platelet-rich fibrin (L-PRF) samples were processed at 2700 rpm for 12 minutes (~700 RCF-max) [17] using an

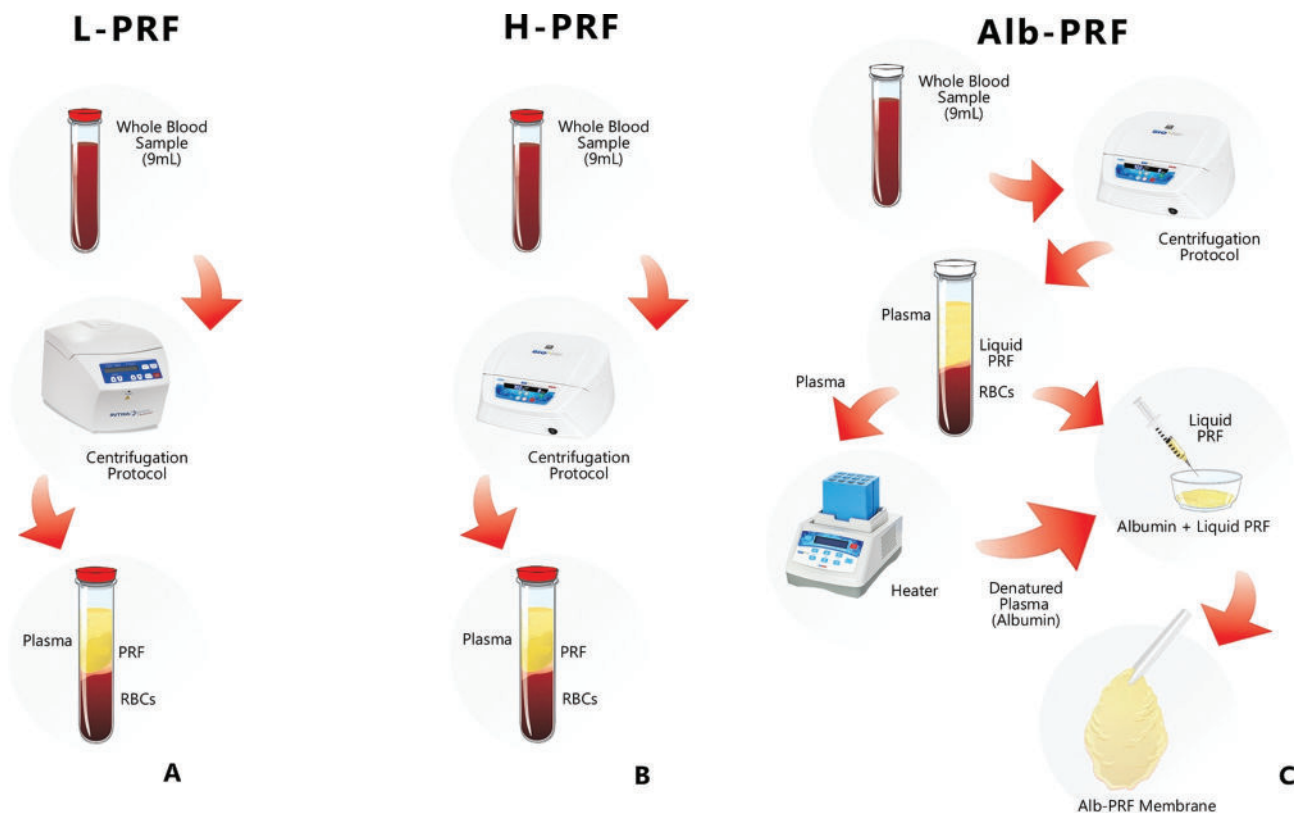


Figure 1. Scheme for PRF membranes production. a. For L-PRF samples production the whole blood was collected and processed at 2700 rpm for 12 minutes; b. For H-PRF samples production the whole blood was collected and processed in a horizontal centrifugation, at 700 RCF-max for 8 minutes, and c. For Alb-PRF samples production the whole blood samples were collected and the protocol for H-PRF was applied to obtain the liquid phase (plasma + portion rich in cells)—8 minutes centrifugation at 700 RCF-max. Approximately 2 ml of plasma was collected and inserted into a device for the human plasma denaturation of proteins for 10 minutes at a temperature of 75°C. Subsequently, 4 ml of the rich portion from the buffy coat layer was collected, added to the heated PPP layer in the glass container, and gently mixed. After 5 min the membrane was formed.

Intraspin centrifuge (Biohorizons, Alabama, USA). Horizontal centrifugation (H-PRF), at 700 RCF-max for 8 minutes (Eppendorf 5702, Hamburg, Germany), was also used to produce PRF (Figure 1a-b).

Preparation of Alb-PRF Membranes

The same blood donor was utilized for the production of Alb-PRF. Whole blood samples were collected using plastic PET tubes without any additives. To produce each membrane, two tubes were placed in a horizontal rotor centrifuge (Bio-PRF, Venice, Florida, USA), and the protocol for H-PRF was applied to obtain the liquid phase (plasma + portion rich in cells)—8 minutes centrifugation at 700 RCF-max. After processing, it was possible to use the plasma and remaining decanted blood material containing red cells.

Approximately 2 ml of the initial portion of plasma was collected using a syringe with an 18 G needle (Injex®, São Paulo, Brazil), while the rest of the blood (portion rich in cells, and red blood cells) was preserved at room temperature (20°C). The syringes containing platelets poor plasma (PPP) were inserted into a device for the human plasma denaturation of proteins (Bio-Heat, Bio-PRF, Venice, Florida, USA). After 10 minutes at a temperature of 75°C, the syringes were stored at room temperature for another 10 minutes to allow cooling (as recommended by the manufacturer).

Subsequently, using a 10 ml syringe with an 18 G needle (Injex®, Brazil), the 4 ml of the rich portion from the buffy coat layer was collected, added to the heated PPP layer in the glass container, and gently mixed. After the fibrin polymerization process was complete (approximately 5 min), the membrane was formed (Figure 1c).

Animal Characterization and Experimental Group

In this study, 30 female nude mice were used, aged between 30 and 40 days old, weighing 20 to 30 grams, and were provided by the Laboratory Animal Center (NAL) located at the Fluminense Federal University, Niterói, Brazil. Nude mice were used because they are deficient in T lymphocytes. Therefore, the animals do not reject transplants from other lineages or species. They have been widely used in various other studies and demonstrated good compatibility with implanted biomaterials [8,18,19].

Before and after the experimental periods, the animals were kept in isolators—with a maximum of 5 animals in each—and were fed pelleted feed and water *ad libitum*. A senior veterinarian monitored the nutritional parameters, animal care, and pre- and post-operative fasting of the animals.

The animals were divided into four groups with equal PRF membrane size (1 cm × 0.5 cm)—Group 1: Sham (without membrane implantation); Group 2: L-PRF; Group 3: H-PRF; and Group 4: Alb-PRF. All experimental groups were further subdivided according to their experimental period (7, 14, and 21 days), with five animals in each group's experimental period.

Surgical Procedures

All aspects of animal care and accommodation were performed in accordance with ISO 10993-2 and ISO 10993-6. Several biological response parameters were assessed and recorded, included the following:

- (1) The extent of the fibrosis capsule layer and inflammation, measured semiquantitatively (see Table I).
- (2) The degeneration, determined by assessing changes in tissue morphology.
- (3) the number and distribution of inflammatory cells, namely, polymorphonuclear cells, lymphocytes, plasma cells,

Table I. Semi-quantitative histological evaluation system — Cell type/response.

Cell type/response	Score				
	0	1	2	3	4
Polymorphonuclear cells	0	Rare, 1 to 5/ phf	5 to 10/ phf	Heavy infiltrate	Packed
Lymphocytes	0				
Plasma cells	0				
Macrophages	0				
Giant cells	0	Rare, 1 to 2/ phf	3 to 5/ phf		Sheets
Necrosis	0	Minimal	Mild	Moderate	Severe

- eosinophils, macrophages, and multinucleated cells, as a function of distance from the material–tissue interface.
- (4) The presence and extent of necrosis.
- (5) Other tissue alterations, such as vascularization, fatty infiltration, granuloma formation, mineralization, and bone formation.
- (6) Material parameters, such as fragmentation or the presence of debris, including the form and location of the degraded material.
- (7) The quality and quantity of tissue ingrowth for porous and absorbable implant materials.

Before conducting surgical procedures, all animals were fasted for 24 hours and were administered general anesthesia intraperitoneally, following the protocol of the Fluminense Federal University, using a 0.6-mL injection of the anesthetic solution prepared with 1.0 mL of 10% ketamine (Dopalen®-100 mg/mL), 0.5 mL of 2% xylazine (Anasedan® 20 mg/mL), and 8.5 mL of sterile saline (KabiPac®).

Three minutes later, degermation was performed using chlorhexidine degermant and chlorhexidine alcoholic 2% solutions (Riohex Scrub®, Rioquímica; São José do Rio Preto, São Paulo, Brazil). An approximately 1-cm-long incision was made in the epithelium of the animal's dorsal region, followed by divulsion of the muscular fascia using a scalpel and blunt-tipped scissors to expose the subcutaneous tissue to facilitate insertion of the membrane (1 cm × 0.5 cm) into the subcutaneous region. This was followed by 5–0 nylon suturing (Technofio, Permed, Mafra, Santa Catarina, Brazil) and antisepsis using gauze and alcoholic chlorhexidine solution in the postoperative period. The animals were housed at the Animal Experimentation Laboratory (AEL/UFF) and separated into different mini isolators based on their experimental groups, where they received food and water *ad libitum* (Figure 1). On the day of the surgery and on each of the following two days, 5 mg/kg of Meloxicam (Eurofarma Laboratórios LTDA, São Paulo, SP, Brazil) was administered subcutaneously every 24 h. All animals were observed daily to evaluate and record any postoperative complications.

The mice were euthanized after their respective experimental periods with lethal doses of anesthetic solution and samples—along with adjacent subcutaneous tissue (±5 mm with safety margins)—were collected, fixed, dehydrated, clarified, and placed in paraffin to obtain 5-µm thick slices. The slices were stained with hematoxylin and eosin (HE) and observed using a light field microscope at 40× magnification (OLYMPUS BX43, Tokyo, Japan). These images were captured using a high-resolution digital camera (OLYMPUS SC100, Tokyo, Japan) with a 10× and 40× Acroplan objective lens at the Laboratory of Applied Biotechnology—UFF (LABA, Niterói, Brazil) for descriptive and semiquantitative histological evaluation regarding the

presence of inflammatory infiltrate, vascular neoformation, extension and type of necrosis, presence of fatty infiltrate, fibrosis, and membrane resorption.

Structural Analysis by SEM and Histological Evaluation

Immediately after production, the L-PRF, H-PRF, and Alb-PRF membranes were cut into two pieces and one was fixed with Karnovsky's solution and post-fixed with 0.2 M sodium cacodylate solution and 1% osmium tetroxide solution. It was sequentially dehydrated in alcohol solutions (15% to 100%) and hexamethyldisilazane (HMDS), followed by metalizing with gold and observation at 15 kV using a scanning electron microscope (JEOL JSM-6490 LV, JEOL, Japan).

Descriptive histological analysis was performed for all samples, followed by semiquantitative analysis, in accordance with ISO 10993–6 (Table I and 2). In this semiquantitative scheme, inflammatory cell infiltrates and necrosis were scored using the scoring scheme shown in Table I. Neovascularization, fibrosis, and fatty infiltration are scored using the scoring scheme shown in Table II. According to ISO 10993–6 standards, owing to the greater importance of inflammatory cell infiltrates and necrosis—in comparison to neovascularization, fibrosis, and fatty infiltration parameters—when calculating the total tissue response of each of the implanted materials, these parameters were multiplied by a factor of 2 to provide a weighted value (see Table II). In the supplementary Table I, the totaled values are shown, along with an average score for test and control treatments. Statistical analysis was performed using two-way ANOVA with a Bonferroni test

using the GraphPad Prism software. All data were compared to the control L-PRF group.

Evaluation of Growth Factor Release

To determine the ability to release growth factors (L-PRF, H-PRF, and Alb-PRF), membranes ($n = 3$ per group) were incubated in 6-well culture plates (TPP, USA) in the presence of 4 ml of DMEM (Dulbecco's Modified Eagle's Medium, GIBCO, USA) without antibiotics, in a humidified atmosphere at 37°C/5% CO₂. The conditioned culture media were collected after 7 days of culture and stored at –80°C. For the detection of growth factors, conventional enzyme-linked immunosorbent assay (ELISA) was employed using commercial kits (Peprotech, Rocky Hills, NJ). Assays were performed for the presence of FGF2, VEGF, and PDGF-bb in three independent experiments with five technical replicates. The final optical density was measured using a Synergy II Microplate Reader (Biotek, USA).

Statistical Analysis

After a D'Agostino–Pearson normality test, the results of the ELISA assays were compared using one-way ANOVA with a Tukey post-hoc test. Results regarding alterations in the membrane area with time after implantation were evaluated using two-way ANOVA with a Dunnett's multiple comparisons test, considering an alpha error of 5%, using the software GraphPad Prism 7.0 (GraphPad®, USA).

Table II. Semi-quantitative histological evaluation system — Tissue response.

Response	Score				
	0	1	2	3	4
Neovascularisation	0 Minimal capillary proliferation, focal, 1 to 3 buds	Groups of 4 to 7 capillaries with supporting fibroblastic structures	Broad band of capillaries with supporting fibroblastic structures	Extensive band of capillaries with supporting fibroblastic structures	
Fibrosis	0 Narrow band	Moderately thick band	Thick band	Extensive band	
Fatty infiltrate	0 Minimal amount of fat associated with fibrosis	Several layers of fat and fibrosis	Elongated and broad accumulation of fat cells about the implant site	Extensive fat completely surrounding the implant	

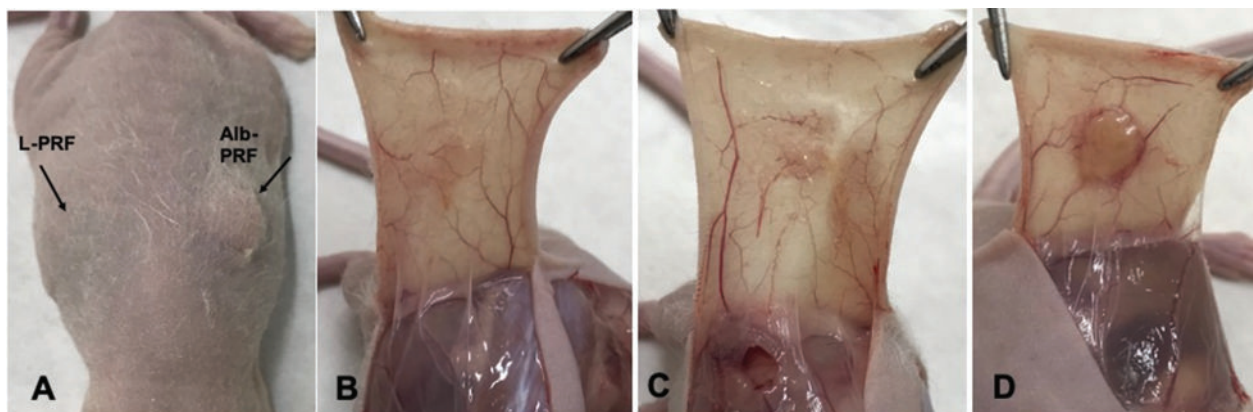


Figure 2. After 21 days of implantation, macroscopically, it was observed the volume on the animal's back, referring to the ALB-PRF, which remained in place during all the experimental periods. A. Animal's back with ALB-PRF volume (arrow); B. L-PRF; C. H-PRF; D. Alb-PRF.

Figure 3. Quantification of the membrane surface area. Both the L-PRF and H-PRF groups noted complete resorption by day 21. Alb-PRF demonstrated superior volume stability over time ($p < .05$; * significantly greater surface area when compared to all other groups).

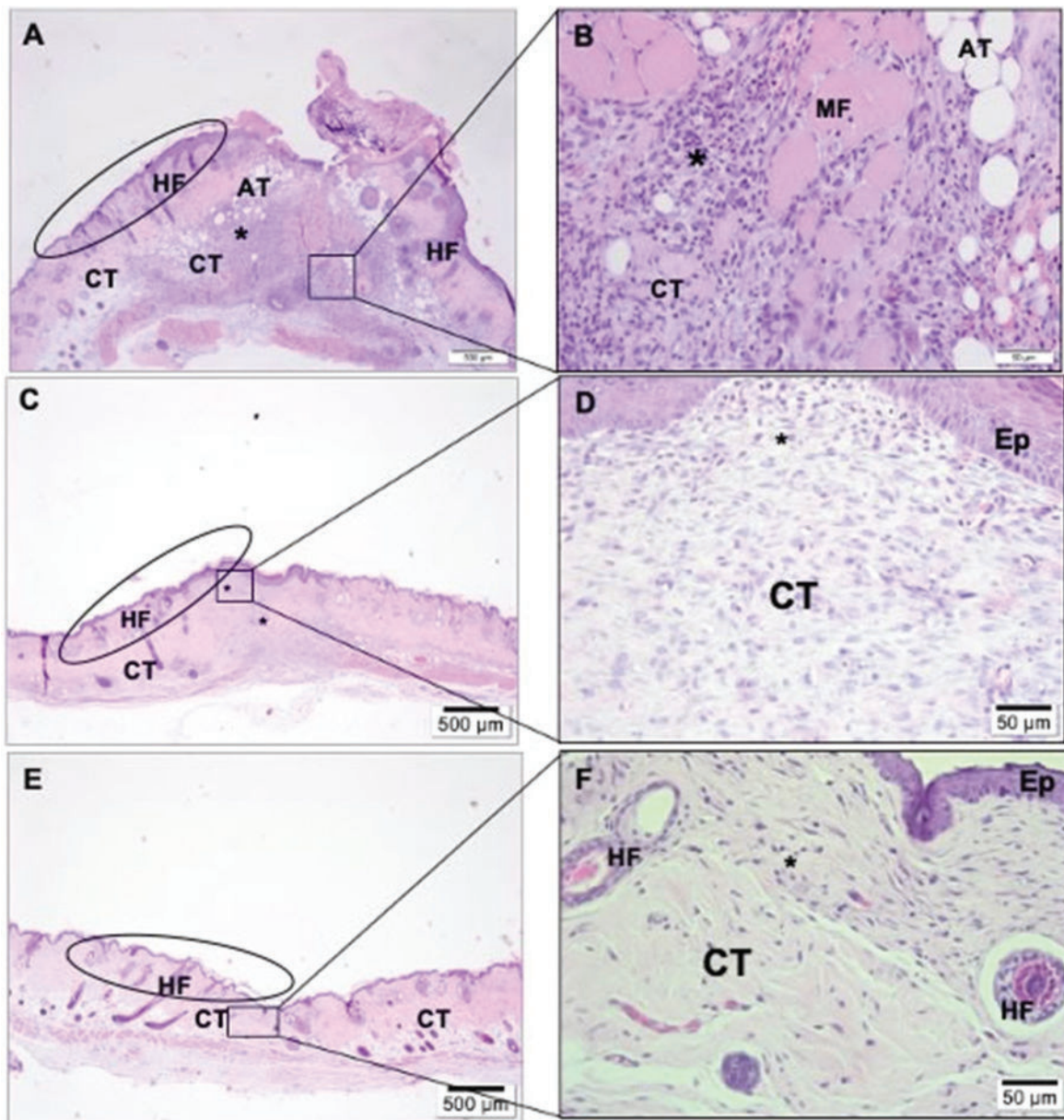
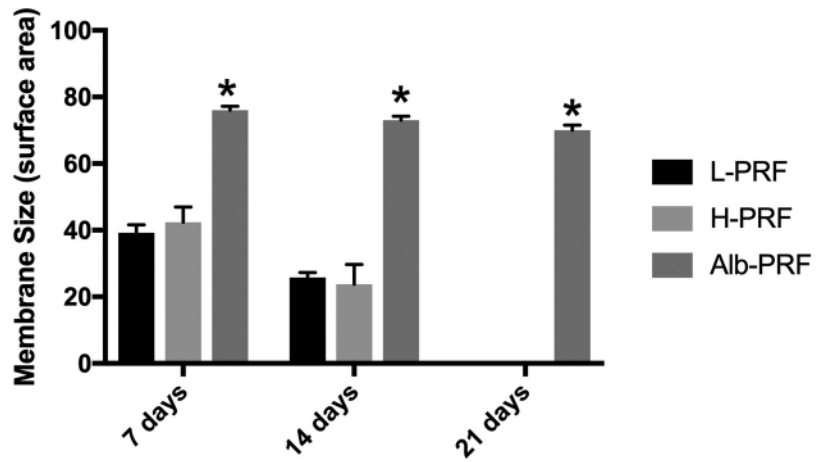


Figure 4. Photomicrographs of Sham Group. A and B circle: epidermis and papillary dermis with hair follicle (HF), recovering connective tissue (CT) with focal intense and diffuse inflammatory cells (*); muscle fibers (MF) and adipocyte tissue (AT) are noted. C and D: circle: epidermis (EP) and papillary dermis with hair follicle (HF), recovering connective tissue (CT) with moderate focal inflammatory cells (*). E and F: circle: epidermis (EP) and papillary dermis with hair follicle (HF), recovering connective tissue (CT). Rare inflammatory cells (*) are noted. A and B: 7 days; C and D: 14 days; E and F: 21 days. A, C and E: 40 x magnification, scale bar: 500 μ m; B, D and F: 400 x magnification, scale bar: 50 μ m. Stain: Hematoxylin and Eosin.

Results

Histological Evaluation after Implantation

The biological response was evaluated by assessing the tissue response (neovascularization, fibrosis, and fatty infiltrate) and the presence of inflammatory cells (polymorphonuclear cells, lymphocytes, plasma cells, macrophages, giant cells, and necrosis) as a function of time. The test sample response was compared to that obtained from the control sample site. After 21 days, it was macroscopically observed that the majority of samples implanted with L-PRF or H-PRF demonstrated significant or complete resorption, whereas the Alb-PRF group demonstrated only a slight change in volume dimensions (Figure 2). Figure 2a shows an animal that was subcutaneously implanted

on either side of the animal midline with L-PRF and Alb-PRF. Note the complete resorption of the L-PRF group; however, a bolus remained in the opposite Alb-PRF group (Figure 2a). Figure 2b-d further shows that the L-PRF and H-PRF group demonstrated complete resorption at day 21. The Alb-PRF group exhibited vascularization around the implanted biomaterial with notable volume-stability over the entire study duration (Figure 2d).

Quantification of the membrane size surface area demonstrated that both the L-PRF and H-PRF groups lost approximately 50% volume in comparison to the Alb-PRF group in 7 days. Roughly 25% of the volume was lost by day 14 and complete resorption was noted by day 21 for the L-PRF and H-PRF groups (Figure 3). In contrast, from day 7 to day 21, the Alb-PRF group

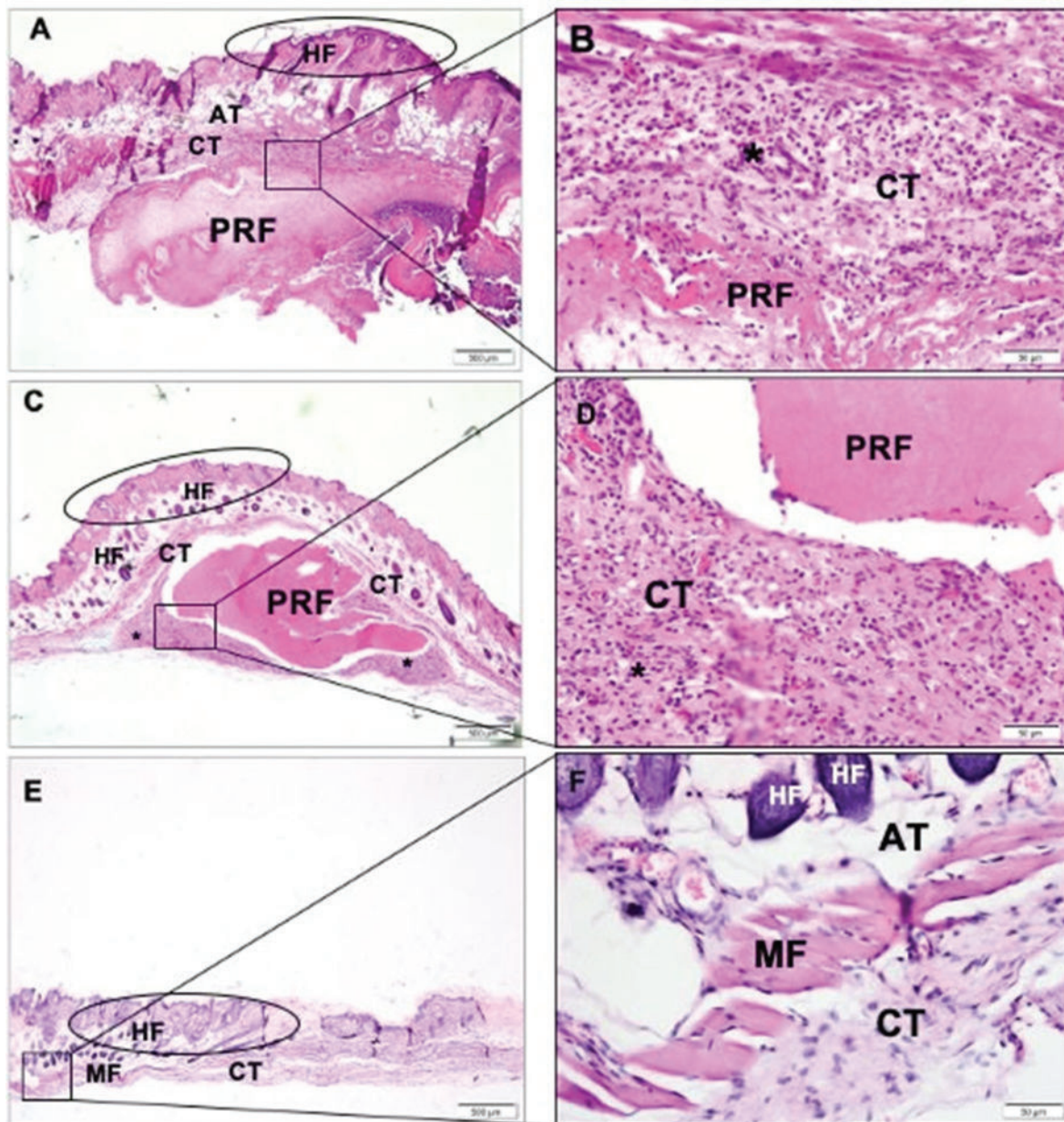


Figure 5. Photomicrographs of L-PRF group. a and b: circle: epidermis and papillary dermis with hair follicle (HF), recovering connective tissue (CT) with moderate and diffuse inflammatory cells (*) surrounding PRF (PRF). adipocyte tissue (AT) are noted above the epithelium. c and d: circle: epidermis and papillary dermis with hair follicle (HF), recovering connective tissue (CT) with moderate and diffuse inflammatory cells (*) surrounding PRF (PRF). E and F: circle: epidermis and papillary dermis with hair follicle (HF), recovering connective tissue (CT). rare inflammatory cells among muscle fibers (mf) and adipocyte tissue (AT) are noted. PRF was not observed in this period. a and b: 7 days; c and d: 14 days; e and f: 21 days. a, c and e: 4 x magnification, scale bar: 500 μ m; b, d and f: 40 x magnification, scale bar: 50 μ m. Stain: Hematoxylin and Eosin. a and b: 7 days; c and d: 14 days; e and f: 21 days. a, c and e: 40 x magnification, scale bar: 500 μ m; b, d and F: 400 x magnification, scale bar: 50 μ m. Stain: Hematoxylin and Eosin.

lost approximately 10% of its original volume, demonstrating superior volume stability over time (Figure 3).

Sham Group

After seven days, the absence of fibrosis and fatty infiltrate was observed with minimal focal capillary proliferation, from 1 to 3 buds per field. The semiquantitative scores for polymorphonuclear cells, lymphocytes, and macrophages were moderate; giant cells and plasma cells were rare; and there was a total absence of necrosis (Figure 4a-b).

After 14 days, fibrosis, fatty infiltrate, and necrosis were absent; further, minimal focal capillary proliferation—from 1 to 3 buds per field—was observed. There was only a slight presence of inflammatory cells, such as polymorphonuclear cells and

plasma cells; rare to moderate presence of lymphocytes and macrophage cells; and an absence of giant cells (Figure 4c-d).

After 21 days, the inflammatory cells were absent, and lymphocytes and macrophage cells were rare. Further, fibrosis, necrosis, and fatty infiltrate were absent, while the presence of minimal focal capillary proliferation, from 1 to 3 buds per field, was observed (Figure 4e-f).

L-PRF Group

After 7 days, the absence of giant cells and rare presence of plasma cells was observed; however, the infiltration of polymorphonuclear cells, lymphocytes, and macrophage cells was moderate. A group of 4 to 7 capillaries—along with supporting fibroblastic structures—was seen for each evaluated field, characterizing moderate neovascularization (Figure 5a-b). After

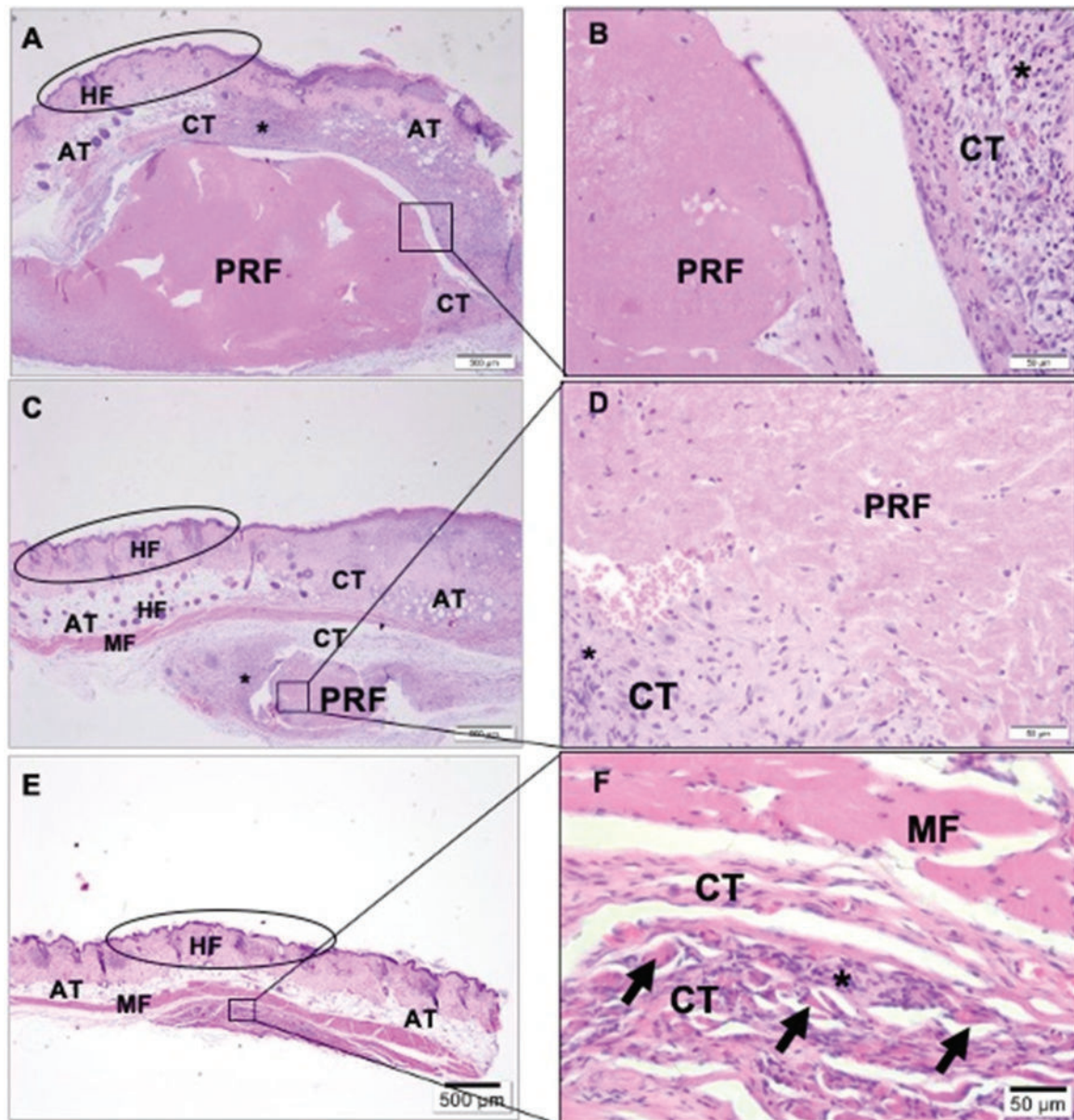


Figure 6. Photomicrographs of H-PRF group. a and b: circle: epidermis and papillary dermis with hair follicle (HF), recovering connective tissue (CT) with intense and diffuse inflammatory cells (*) surrounding PRF (PRF). adipocyte tissue (AT) are noted above the epithelium. c and d: circle: epidermis and papillary dermis with hair follicle (HF), recovering connective tissue (CT) with moderate focal inflammatory cells (*) surrounding PRF (PRF), muscle fibers (MF) and adipocyte tissue (AT) are noted. e and f: circle: epidermis and papillary dermis with hair follicle (HF), recovering connective tissue (CT). focally inflammatory cells streaky muscle fibers (arrow). PRF was not observed in this period. a and b: 7 days; c and d: 14 days; e and f: 21 days. a, c and e: 40x magnification, scale bar: 500 μ m; b, d and f: 400x magnification, scale bar: 50 μ m. Stain: Hematoxylin and Eosin.

14 days of implantation, the presence of lymphocytes and macrophages was constant, while a decrease in polymorphonuclear and plasma cells was detected in comparison to the 7-day group. Tissue reactions such as necrosis, fibrosis, and fatty infiltrates were not observed, and minimal capillary proliferation was observed (1 to 3 buds per field) (Figure 5c-d). After 21 days, it was observed that all inflammation cells decreased significantly owing to the resorption of the L-PRF membrane. The exception to this was lymphocytes which—although rare—were present (Figure 5e-f).

H-PRF Group

The results of the L-PRF group and H-PRF group were comparable with respect to biocompatibility and inflammatory response. After 7 days of implantation, a moderate presence of polymorphonuclear and macrophage cells was observed, while plasma cells were rare and giant cells and necrosis were absent (Figure 6a-b). The reduction in the number of inflammatory cells was time-dependent over the study period. By day 21, fewer cells were observed and less neovascularization (from moderate to rare) was

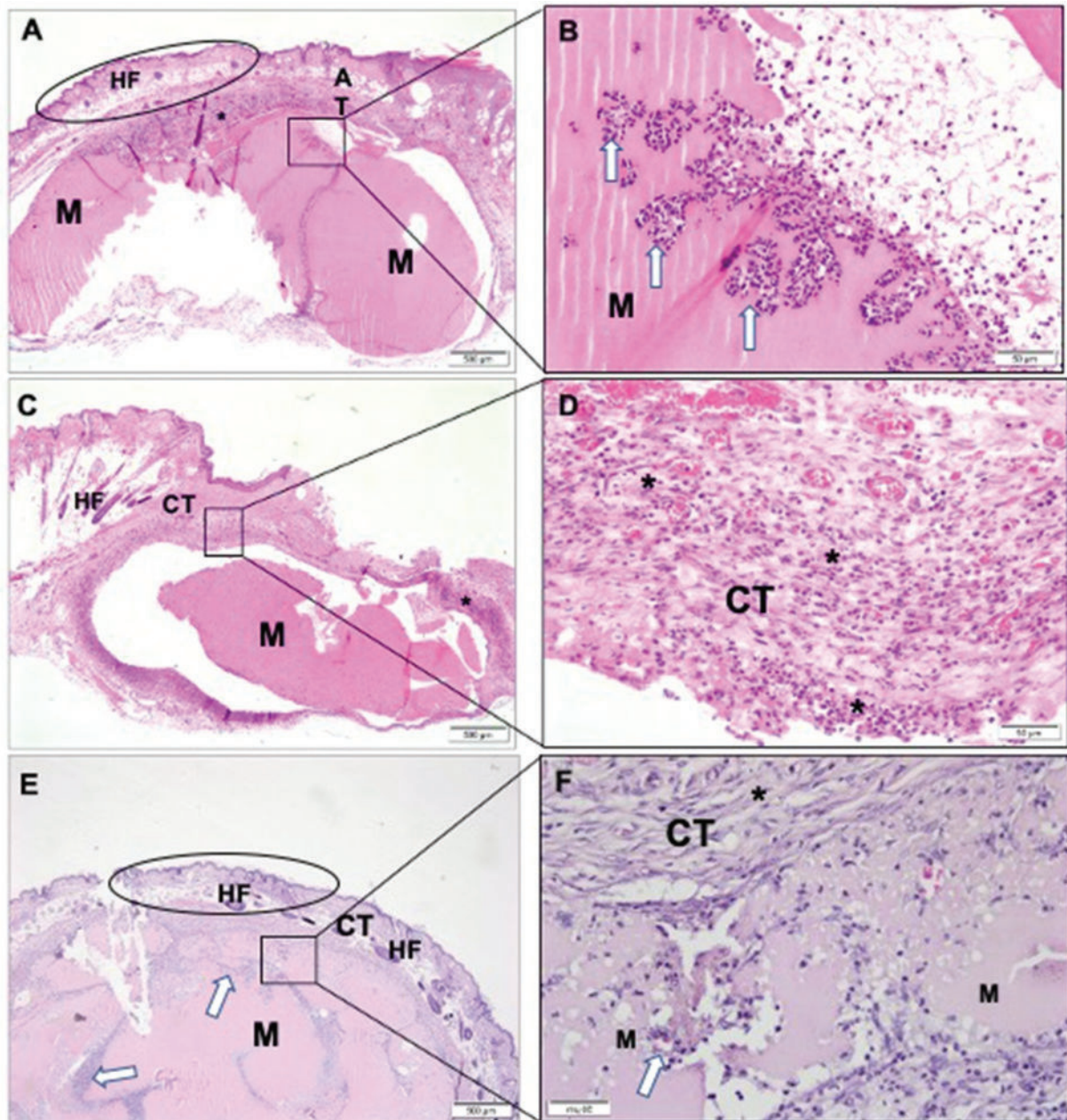


Figure 7. Photomicrographs of Alb-Prf group. a and b: circle: epidermis and papillary dermis with hair follicle (HF), recovering connective tissue (CT) with moderate and focal inflammatory cells (*) surrounding PRF (PRF). Highlighting the presence of leukocyte groups inside the membrane (white arrow); c and d: circle: epidermis and papillary dermis with hair follicle (HF), recovering connective tissue (CT) with moderate inflammatory cells (*) surrounding PRF (PRF); E and F: circle: epidermis and papillary dermis with hair follicle (HF), recovering connective tissue (CT) with disperse inflammatory cells (*) surrounding PRF); presence of leukocyte groups inside the membrane (white arrow) a and b: 7 days; c and d: 14 days; e and f: 21 days. a, c and e: 40 x magnification, scale bar: 500 μ m; B, D and F: 400 x magnification, scale bar: 50 μ m. Stain: Hematoxylin and Eosin.

Table III. Semi-quantitative evaluation utilized to evaluate the tissue reaction and biocompatibility as highlighted in ISO 10993–6. The present example are for the 5 animals evaluated at 7 days for the L-PRF group. 5 sections were evaluated per animal.

7 days	Animal 1					Animal 2					Animal 3					Animal 4					Animal 5				
L-PRF	1	2	3	4	5	1	2	3	4	5	1	2	3	4	5	1	2	3	4	5	1	2	3	4	5
Polymorphonuclear cells	2	2	3	3	3	2	2	1	3	2	2	2	1	2	1	2	2	3	3	1	2	1	1	2	2
Lymphocytes	2	2	2	2	2	2	2	1	2	2	2	2	2	2	2	1	3	2	2	2	2	2	2	2	2
Plasma cells	2	1	1	1	1	0	1	1	1	1	1	2	1	1	2	1	1	0	1	1	1	1	2	2	1
Macrophages	2	1	2	2	2	2	2	1	2	2	2	2	3	1	1	3	3	3	3	1	1	1	1	1	1
Giant cells	0	0	0	0	0	0	0	0	0	0	0	0	0	0	0	0	0	0	0	0	0	0	0	0	0
Necrosis	0	0	0	0	0	0	0	0	0	0	0	0	0	0	0	0	0	0	0	0	0	0	0	0	0
Score from inflammatory cells	Sum = 8, 8, 8, 8, 8					Sum = 6, 7, 4, 8, 7					Sum = 7, 8, 7, 6, 7, 6					Sum = 7, 9, 8, 9, 5					Sum = 6, 6, 6, 7, 6				
SUBTOTAL (X 2)	16, 16, 16, 16, 16					12, 14, 8, 16, 14					14, 16, 14, 12, 14, 12					14, 18, 16, 18, 10					12, 12, 12, 14, 12				
Neovascularisation	1	2	1	1	2	2	3	0	3	3	1	2	2	1	1	1	1	1	2	2	0	1	2	1	1
Fibrosis	0	0	0	0	0	0	0	0	0	0	0	0	0	0	0	0	0	0	0	0	0	0	0	0	0
Fatty infiltrate	0	0	0	0	0	0	0	0	0	0	0	0	0	0	0	0	0	0	0	0	0	0	0	0	0
SUB-TOTAL from tissue response	1	2	1	1	2	2	3	0	3	3	1	2	2	1	1	1	1	1	2	2	0	1	2	1	1
TOTAL	17	18	17	17	18	14	17	8	19	17	15	18	16	15	13	15	19	17	20	12	12	13	14	15	13
AVERAGE	17.4					15					15.4					16.6					13.4				

present (Figure 6c-f). It is important to note that the degradation of the L-PRF membrane occurred slightly faster than that of the H-PRF membrane, resulting in the presence of more inflammatory cells at 21 days when comparing both groups.

Alb-PRF Group

After 7 days, fewer inflammatory cells were observed for all cell types in this group. Few macrophages and giant cells, along with the presence of neovascularization was observed at this early time (Figure 7a-b). After 14 days, the number of inflammatory cells gradually increased in a similar manner to other groups (Figure 7c-d). By 21 days, the number of inflammatory cells continued to decrease, along with the local neovascularization (Figure 7e-f). Fibrosis, necrosis, fatty infiltrate, and giant cells were not reported in this group. It is also worth noting that, in comparison to other groups, the Alb-PRF group was relatively stable, with little resorption over time.

Semi-Quantitative Analysis according to ISO Standard 10993-6

Following a descriptive analysis of the implanted PRF membranes, a semi-quantitative evaluation system that used scoring was implemented in accordance with ISO 10993–6. Table III demonstrates a sample evaluation of the L-PRF group at 7 days (all data can be found in supplementary Table I). Scoring was conducted in accordance with ISO standards whereby the tissue inflammatory response can be observed and compared with that of other groups. Figure 8 demonstrates the inflammatory responses of inflammatory cells (Figure 8a-f), along with the overall tissue reaction (Figure 8g-h), with the final calculated outcomes reported in Figure 8i. Note that, owing to the autologous nature of PRF, all groups responded extremely favorably—with only mild increases in inflammation—in comparison to the negative Sham control (Figure 8).

Membrane Characterization

The ultrastructural evaluation of the membranes was performed using SEM, as shown in Figure 9. The PRF membrane is characterized as a dense fibrin network with close-knit frames, similar to gauze threads, which entrap cells among the fibers (Figure 9a). The H-PRF membrane was similarly characterized by a fibrin mesh; however, it had an increased presence of entrapped cell elements (Figure 9b). The Alb-PRF membranes demonstrated

a very dense surface with evident deposition of a layer of denatured protein that completely coated the fibrin fibers and surrounded entrapped cells and platelets (Figure 9c).

The capacity of the membranes for the retention or production of growth factors was assessed through an *in vitro* elution assay. Figure 10 demonstrates the growth factor release of PDGF, VEGF, and FGF2 after 7 days of elution in the culture medium. While the mean release of FGF2 from all groups was similar, a significantly higher release ($p < .05$) of VEGF and PDGF was observed in the H-PRF group, with final concentrations approximately two-fold higher than those found for the L-PRF and Alb-PRF groups (Figure 10).

Discussion

The aim of GBR is to exclude faster-growing soft tissue cells from the underlying bony tissue. To accomplish this, adequate space maintenance over a 2–3 month period is required[4]. Animal-based collagen-barrier membranes are most frequently utilized owing to their biocompatibility with human tissue. Nevertheless, alternative strategies with either better membrane stability or biocompatibility are necessary to further improve clinical outcomes.

Platelet-rich fibrin has previously been utilized as a regenerative barrier membrane for various GBR procedures. It has the advantage of being completely autologous but further stimulates tissue regeneration in both hard and soft tissue by improving their vascularization *in vivo* [20–22]. Nevertheless, while PRF does offer greater regenerative potential, it degrades quite rapidly *in vivo*, within the first 2–3 weeks post-implantation. For these reasons, many authors have recommended coating collagen membranes either directly with liquid-PRF or laying a standard PRF membrane over the top of an animal-derived barrier membrane[23].

More than 20 years have passed since it was shown that, by heating and denaturing albumin, a modification in the secondary structure transforms the albumin into a tridimensional structure, whereby new hydrogen and disulfide ligations in the enzymes are created[24]. This favors a larger tridimensional structure with drastic changes in its resorption properties and improved stability over time. [24]

Previous studies have already studied the change in temperature for the production of fibrin membranes [8,12,13,25]. In 2015, Kawase et al. investigated the degradation properties of PRF. By

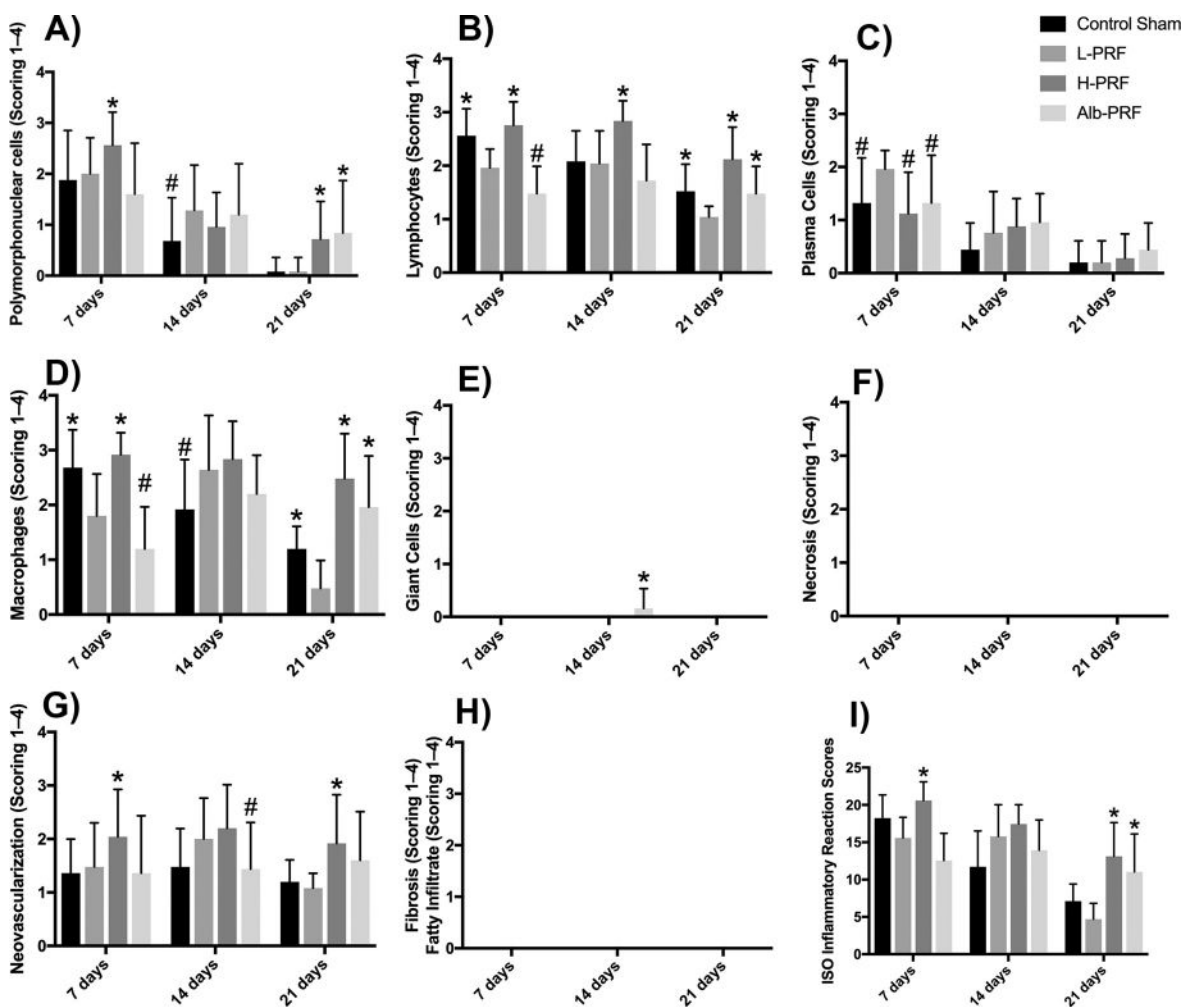


Figure 8. Inflammatory cells response (8A-F) and overall tissue reaction. (8 G, H) with the final calculated outcomes reported in I. Note that all groups responded extremely favorably with only mild increases in inflammation when compared to the negative Sham control (data \pm standard deviation; $p < .05$; * represents significantly greater when compared to the control L-PRF group; #represents significantly lower when compared to the L-PRF group).

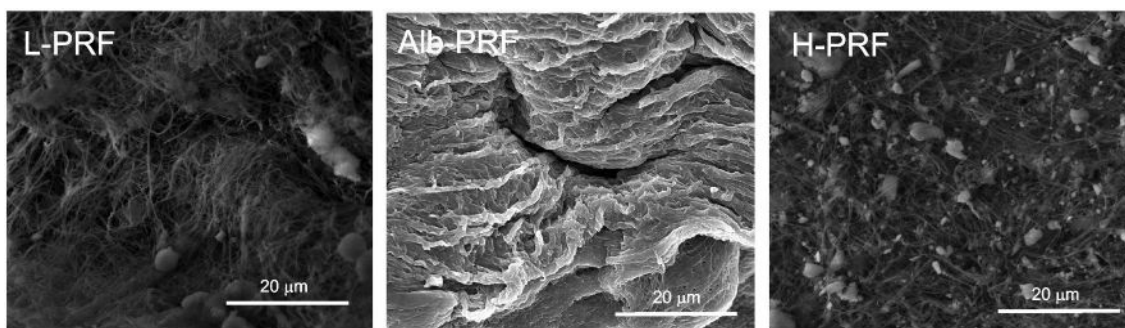


Figure 9. Scanning electron micrographs of the (a) L-PRF, (b) H-PRF and (c) Alb-CGF membranes obtained with a scanning electron microscope (JEOL JSM-6490 LV, JEOL, Japan) at 15 kV.

applying heat treatment to standard PRF membranes through membrane compression, the resorption properties of PRF membranes were dramatically improved[8]. While benefits were reported in terms of its stability, one of the limitations was the fact that, during the heating process, cells typically go through apoptosis and growth-factor activity is dramatically reduced during their denaturation.

A recent research discussed the need to improve the handling of PRF since it had fast degradation properties with low tensile strength [25]. They therefore produced a sterile, saturable PRF membrane by creating a single-syringe closed system (hypACT Inject) to produce a PRF membrane with better handling characteristics by a freeze-thawing method. They found significantly

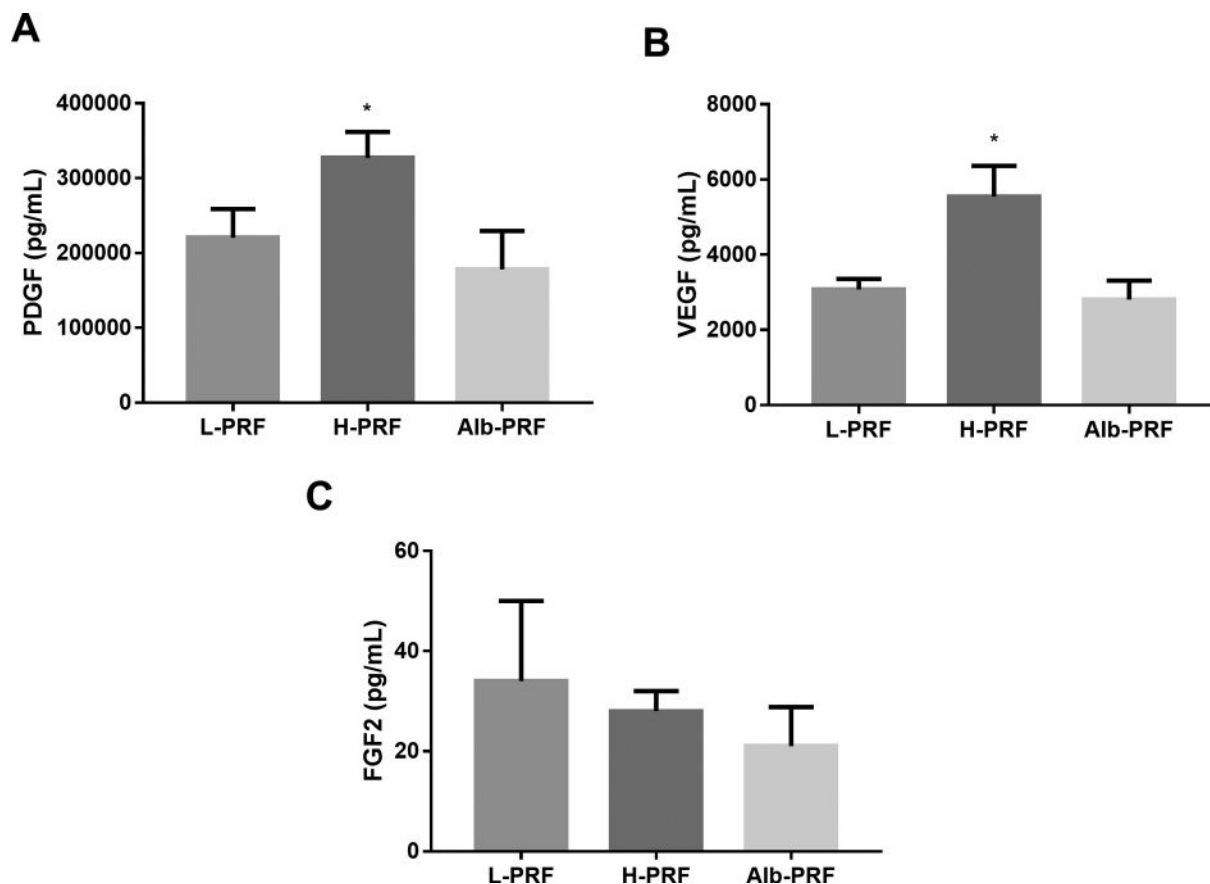


Figure 10. Assessment of the release of growth factors PDGF (A), VEGF (B) and FGF2 (C) from the L-PRF, H-PRF and Alb-PRF group respectively after 7 days of elution into cell culture media. Bars represent the mean \pm SD of three biological and five technical replicates. An asterisk indicates a statistically significant difference between groups ($p < .005$).

higher tensile strength, higher cell adhesion and a lower degradation rate of the membranes.

Unlike any previously produced PRF, Mourão et al proposed the utilization of the PPP layer as the heat-treated component with extended PRF-resorption properties, along with advantages such as membrane stability over time[12]. However, this needed to be done while ensuring the retention of cells from the buffy coat layer and using growth factors to maintain the regenerative properties of PRF within the heated PPP layer[12]. It has also been shown that these membranes retain their ability to release growth factors over an extended period of time, favoring fibroblast migration and proliferation, along with inducing collagen synthesis[13]. In this study, it was once again observed that the release of growth factors from Alb-PRF was similar to that from L-PRF and that the H-PRF group demonstrated significantly higher levels of growth factor than either group[26].

The main aim of this study was to investigate the *in vivo* biocompatibility and stability of Alb-PRF membranes in comparison to two standard protocols utilized for the production of PRF. It was found that all PRF membranes demonstrated excellent biocompatibility, similar to the negative control (Sham group). However, it is noteworthy that, while standard L-PRF and H-PRF protocols demonstrated a reduction in membrane size between 7 and 14 days—and near-complete resorption by 21 days—it was observed that the Alb-PRF membrane maintained its volume stability even at 21 days. Further, it should be noted that small rodents have an extremely fast metabolic rate in comparison to humans; therefore, the ability to maintain volume stability even after 21 days correlates well with reports demonstrating months

of volume stability of Alb-PRF when it is used as a biological filler or barrier membrane.

The extended resorption properties of Alb-PRF have numerous advantages in a variety of clinical procedures. Furthermore, the additional processing adds only 10–20 minutes to the current protocol time for regular PRF. Based on these observations, it is possible to create a true “barrier” or “filler” biomaterial derived from 100% autologous whole blood, with drastically improved resorption properties. Furthermore, the ability to easily collect several vials of 10 mL blood samples makes this biomaterial extremely useful, especially for harvesting from peripheral veins at a low cost. It is currently being investigated in clinical practice for use during large GBR procedures in dentistry with a titanium mesh. Reports have demonstrated up to a 50% exposure rate of titanium [27–30]. While practicing clinicians have utilized standard PRF over titanium to minimize exposure, the ability to create a longer-lasting Alb-PRF membrane will likely provide additional clinical benefits. It also serves as an attractive biomaterial for a number of patients who wish to avoid using animal-derived products and prefer to be treated using more natural autologous solutions. Future clinical research will be pivotal to further understand the full potential and clinical uses of Alb-PRF in medical practice.

This study revealed the excellent biocompatibility of all investigated PRF groups when implanted subcutaneously according to ISO 10993–6. Only a mild inflammatory response was reported for all groups, with comparable outcomes observed between the L-PRF, H-PRF, and Alb-PRF groups. It is worth noting that, within the present study, the use of the

denatured plasma membrane in combination with liquid PRF (Alb-PRF) was sufficiently volume-stable at all times, whereas both the L-PRF and H-PRF groups showed significant or complete resorption by 14 days. This study demonstrates—for the first time, a marked improvement in the membrane stability of Alb-PRF, with significant future potential for use as a biological barrier membrane for GBR procedures and as a biological filler material in various esthetic medical applications. Therefore, it may potentially be utilized in a similar manner as a xenograft biomaterial, such as porcine-derived collagen membranes, with similar degradation properties yet derived 100% from autologous sources. By utilizing the membrane onsite, it retains living cells which would further contribute to tissue regeneration.

It is important to study the presence of albumin in bone tissue healing, as an activator of endogenous progenitor cells, making it a possible effective and safe adjuvant to bone regenerative procedures[31]. This process of incorporating Alb-PRF with biomaterials for bone defects or even its isolated use as a bone substitute will be studied in future *in vivo* studies and RCTs.

Acknowledgements

Authors acknowledge the financial support of the Brazilian government agencies CAPES and FAPERJ (grant number: E-26/202.713/2019).

Funding

This work was supported by the Fundação Carlos Chagas Filho de Amparo à Pesquisa do Estado do Rio de Janeiro [E-26/202.713/2019].

Declaration Of Interest Statement

Richard J Miron declares that he has intellectual properties for the Bio-PRF and Bio-Heat devices utilized in this study. All other authors declare that they have no conflict of interest.

Supplemental Material

Supplemental material for this article can be accessed [here](#).

ORCID

Carlos Fernando de Almeida Barros Mourão  <http://orcid.org/0000-0001-5775-0222>

Adriana Terezinha Alves  <http://orcid.org/0000-0002-3665-6568>

Mônica D. Calasans-Maia  <http://orcid.org/0000-0001-5759-7926>

References

- CFdAB M, Lourenço ES, Nascimento JRB, Machado RCM, Rossi AM, Leite PEC, Granjeiro JM, Alves GG, Calasans-Maia MD. Does the association of blood-derived growth factors to nanostructured carbonated hydroxyapatite contributes to the maxillary sinus floor elevation? A randomized clinical trial. *Clin Oral Investig* 2019;23:369–379. doi:10.1007/s00784-018-2445-7.
- da Costa Pereira L, de Almeida Barros Mourão CF, Alves ATNN, Resende RFB, Uzeda MJ, Granjeiro JM, Louro RS, Calasans-Maia MD. In vitro physico-chemical characterization and standardized *in vivo* evaluation of biocompatibility of a new synthetic membrane for guided bone regeneration. *Materials* 2019;12(7):1186–1195. doi:10.3390/ma12071186.
- Calasans-Maia MD, CFdA M, Alves ATNN, Sartoretto SC, MJP DU, Granjeiro JM. Maxillary sinus augmentation with a new xenograft: a randomized controlled clinical trial. *Clin Implant Dent Relat Res* 2015;17:586–593. doi:10.1111/cid.12289.
- Zhang Y, Zhang X, Shi B, Miron R. Membranes for guided tissue and bone regeneration. *Annals of Oral & Maxillofacial Surgery* 2013;1(1):1–10. doi:10.13172/2052-7837-1-1-451.
- Dohan DM, Choukroun J, Diss A, Dohan SL, Dohan AJ, Mouhyi J, Gogly B. Platelet-rich fibrin (PRF): a second-generation platelet concentrate. Part I: technological concepts and evolution. *Oral Surgery, Oral Medicine, Oral Pathology, Oral Radiology, and Endodontology* 2006;101:37–44.
- Kobayashi E, Fluckiger L, Fujioka-Kobayashi M, Sawada K, Sculean A, Schaller B, Miron RJ. Comparative release of growth factors from PRP, PRF, and advanced-PRF. *Clin Oral Investig* 2016;20(9):2353–2360. doi:10.1007/s00784-016-1719-1.
- Eren G, Gürkan A, Atmaca H, Dönmez A, Atilla G. Effect of centrifugation time on growth factor and MMP release of an experimental platelet-rich fibrin-type product. *Platelets* 2016;27(5):427–432. doi:10.3109/09537104.2015.1131253.
- Kawase T, Kamiya M, Kobayashi M, Tanaka T, Okuda K, Wolff LF, Yoshie H. The heat-compression technique for the conversion of platelet-rich fibrin preparation to a barrier membrane with a reduced rate of biodegradation. *J Biomed Mater Res Part B: Appl Biomater* 2015;103(4):825–831. doi:10.1002/jbm.b.33262.
- de Almeida Barros Mourão CF, Miron RJ, de Mello Machado RC, Ghanaati S, Alves GG, Calasans-Maia MD. Usefulness of platelet-rich fibrin as a hemostatic agent after dental extractions in patients receiving anticoagulant therapy with factor Xa inhibitors: a case series. *Oral and Maxillofacial Surg* 2019;23(3):381–386. doi:10.1007/s10006-019-00769-y.
- CFdAB M, Valiense H, Melo ER, NBMF M, Maia MD-C. Obtention of injectable platelets rich-fibrin (i-PRF) and its polymerization with bone graft. *Revista Do Colégio Brasileiro De Cirurgiões* 2015;42:421–423. doi:10.1590/0100-69912015006013.
- Miron RJ, Zhang Y. Autologous liquid platelet rich fibrin: A novel drug delivery system. *Acta Biomater* 2018;75:35–51. doi:10.1016/j.actbio.2018.05.021.
- Barros Mourão CDA, Gheno E, Lourenço ES, de Lima Barbosa R, Kurtzman GM, Javid K, Mavropoulos E, Benedicenti S, Calasans-Maia MD, de Mello Machado R, de Mello Machado RC. Characterization of a new membrane from concentrated growth factors associated with denatured Albumin (Alb-CGF) for clinical applications: A preliminary study. *Int J Growth Factors and Stem Cells in Dentistry* 2018;1(2):64–69. doi:10.4103/GFSC.GFSC_21_18.
- Fujioka-Kobayashi M, Schaller B, Mourao C, Zhang Y, Sculean A, Miron RJ. Biological characterization of an injectable platelet-rich fibrin mixture consisting of autologous albumin gel and liquid platelet-rich fibrin (Alb-PRF). *Platelets* 2020;20:1–8.
- Kilkenny C, Browne WJ, Cuthill IC, Emerson M, Altman DG. Improving bioscience research reporting: the ARRIVE guidelines for reporting animal research. *PLoS Biol* 2010;8(6):1–10. doi:10.1371/journal.pbio.1000412.
- Smith AJ, Clutton RE, Lilley E, Hansen KEA, Brattelid T. PREPARE: guidelines for planning animal research and testing. *Lab Anim* 2018;52(2):135–141. doi:10.1177/0023677217724823.
- Miron RJ, Dham A, Dham U, Zhang Y, Pikos MA, Sculean A. The effect of age, gender, and time between blood draw and start of centrifugation on the size outcomes of platelet-rich fibrin (PRF) membranes. *Clin Oral Investig* 2018;23:1–7.
- Miron RJ, Pinto NR, Quirynen M, Ghanaati S. Standardization of relative centrifugal forces in studies related to platelet-rich fibrin. *J Periodontology* 2019;90(8):817–820. doi:10.1002/JPER.18-0553.
- Horimizu M, Kubota T, Kawase T, Nagata M, Kobayashi M, Okuda K, Nakata K, Yoshie H. Synergistic effects of the combined use of human-cultured periosteal sheets and platelet-rich fibrin on bone regeneration: an animal study. *Clin Exp Dent Res* 2017;3(4):134–141. doi:10.1002/cre2.71.
- Marsano A, CM MDC, Ghanaati S, Gueven S, Centola M, Tsaryk R, Barbeck M, Stuedle C, Barbero A, Helmrich U. Spontaneous *in vivo* chondrogenesis of bone marrow-derived mesenchymal progenitor cells by blocking vascular endothelial growth factor signaling. *Stem Cells Translational Med* 2016;5:1730–1738.
- El Bagdadi K, Kubesch A, Yu X, Al-Maawi S, Orlowska A, Dias A, Booms P, Dohle E, Sader R, Kirkpatrick CJ, et al. Reduction of relative centrifugal forces increases growth factor release within solid platelet-rich-fibrin (PRF)-based matrices: a roof of concept of LSCC (low speed centrifugation concept). *Eur J Trauma and Emergency Surg* 2019;45(3):467–479. doi:10.1007/s00068-017-0785-7.

21. Halford G, Harrison P, Watson S. Platelets - the second growth cycle.. *Platelets* **2019**;30(1):1–12. doi:[10.1080/09537104.2019.1549810](https://doi.org/10.1080/09537104.2019.1549810).
22. Miron RJ, Zucchelli G, Pikos MA, Salama M, Lee S, Guillemette V, Fujioka-Kobayashi M, Bishara M, Zhang Y, Wang H-L, et al. Use of platelet-rich fibrin in regenerative dentistry: a systematic review. *Clin Oral Investig* **2017**;21(6):1913–1927. doi:[10.1007/s00784-017-2133-z](https://doi.org/10.1007/s00784-017-2133-z).
23. Miron RJ, Pikos MA. PRF as a barrier membrane in guided bone regeneration. *Dent Today* **2017**;21:133–136.
24. Giancola C, De Sena C, Fessas D, Graziano G, Barone G. DSC studies on bovine serum albumin denaturation. Effects of Ionic Strength and SDS Concentration *Int J Biol Macromol* **1997**;20:193–204.
25. Kardos D, Hornyák I, Simon M, Hinsenkamp A, Marschall B, Várdai R, Kállay-Menyhárd A, Pinke B, Mészáros L, Kuten O, et al. Biological and mechanical properties of platelet-rich fibrin membranes after thermal manipulation and preparation in a single-syringe closed system. *Int J Mol* **2018**;19(11):3433. doi:[10.3390/ijms19113433](https://doi.org/10.3390/ijms19113433).
26. Miron RJ, Chai J, Zheng S, Feng M, Sculean A, Zhang Y. A novel method for evaluating and quantifying cell types in platelet rich fibrin and an introduction to horizontal centrifugation. *J Biomed Mater Res Part A* **2019**;107(10):2257–2271. doi:[10.1002/jbm.a.36734](https://doi.org/10.1002/jbm.a.36734).
27. Louis PJ, Gutta R, Said-Al-Naief N, Bartolucci AA. Reconstruction of the maxilla and mandible with particulate bone graft and titanium mesh for implant placement. *J Oral and Maxillofacial Surg: Official J American Association of Oral and Maxillofacial Surgeons* **2008**;66(2):235–245. doi:[10.1016/j.joms.2007.08.022](https://doi.org/10.1016/j.joms.2007.08.022).
28. von Arx T, Kurt B. Implant placement and simultaneous ridge augmentation using autogenous bone and a micro titanium mesh: a prospective clinical study with 20 implants. *Clin Oral Implants Res* **1999**;10(1):24–33. doi:[10.1034/j.1600-0501.1999.100104.x](https://doi.org/10.1034/j.1600-0501.1999.100104.x).
29. Al-Ardah AJ, AlHelal A, Proussaefs P, AlBader B, Al Humaidan AA, Lozada J. Managing titanium mesh exposure with partial removal of the exposed site: a case series study. *J Oral Implantology* **2017**;43(6):482–490. doi:[10.1563/aaid-joi-D-17-00169](https://doi.org/10.1563/aaid-joi-D-17-00169).
30. Maqbool T, Binhammer A, Binhammer P, Antonyshyn OM. Risk factors for titanium mesh implant exposure following cranioplasty. *J Craniofacial Surg* **2018**;29(5):1181–1186. doi:[10.1097/SCS.0000000000004479](https://doi.org/10.1097/SCS.0000000000004479).
31. Horváthy DB, Schandl K, Schwarz CM, Renner K, Hornyák I, Szabó BT, Niculescu-Morza E, Nehrer S, Dobó-Nagy C, Doros A, et al. Serum albumin-coated bone allograft (BoneAlbumin) results in faster bone formation and mechanically stronger bone in aging rats. *J Tissue Eng Regen Med* **2019** Mar;13(3):416–422. Epub 2019 Feb 18. doi:[10.1002/term.2803](https://doi.org/10.1002/term.2803).